CHEMISTRY
AN ASIAN JOURNAL
www.chemasianj.org

Accepted Article

Title: ATI stabilized germylene cation as a cyanosilylation catalyst for aldehydes and ketones

Authors: Vivek Kumar Singh, Dharmendra Singh, Hemant Kumar, Prakash Chandra Joshi, Vishal Singh, Pratima Shukla, Tanu Sharma, Gopalan Rajaraman, and Selvarajan Nagendran

To be cited as: *Chem. Asian J.* **2024**, e202400138

Link to VoR: https://doi.org/10.1002/asia.202400138

A Journal of

ACES
Asian Chemical Editorial Society

WILEY VCH

10.1002/asia.202400138

WILEY VCH

RESEARCH ARTICLE

ATI Stabilized Germylene Cation as a Cyanosilylation Catalyst for Aldehydes and Ketones

Vivek Kumar Singh[a], Dharmendra Singh[a], Hemant Kumar[a], Prakash Chandra Joshi[a], Vishal Singh[a], Pratima Shukla[a], Tanu Sharma[b], Gopalan Rajaraman[b], and Selvarajan Nagendran[a]*

Dedication ((optional))

[a] V. K. Singh, D. Singh, H. Kumar, P. C. Joshi, V. Singh, P. Shukla, and Prof. S. Nagendran*
Department of Chemistry
Indian Institute of Technology Delhi (IIT Delhi)
Hauz Khas, New Delhi, 110016 (India)
E-mail: sisn@chemistry.iitd.ac.in

[b] T. Sharma and G. Rajaraman
Department of Chemistry
Indian Institute of Technology Bombay (IIT Bombay), Mumbai, India

Abstract: The aminotroponiminate (ATI) ligand stabilized germylene cation [(*i*-Bu)$_2$ATIGe][B(C$_6$F$_5$)$_4$] (**2**) is found to be an efficient low-valent main-group catalyst for the cyanosilylation of aldehydes and ketones (ATI = aminotroponiminate). It was synthesized by reacting [(*i*-Bu)$_2$ATIGeCl] (**1**) with Na[B(C$_6$F$_5$)$_4$]. The catalytic cyanosilylation of diverse aliphatic and aromatic carbonyl compounds (aldehydes and ketones) using 0.075–0.75 mol% of compound **2** was completed within 5–45 min. The catalytic efficiency seen with aliphatic aldehydes was around 15,800 h^{-1}, making compound **2** a capable low-valent main-group catalyst for the aldehyde and ketone cyanosilylation reactions. Further, DFT calculations reveal a pronounced charge localization at the germanium atom of compound **2**, leading to its superior catalytic performance.

Introduction

Recent research on main-group chemistry has emphasized the importance of utilizing low-valent main-group element compounds for catalysis.[1] The unique electronic nature of these compounds helps mimic the characteristics of transition metals.[2] Various low-valent main-group element compounds have been used as catalysts for numerous organic transformations, such as cyanosilylation,[3] hydroboration,[4] hydroamination,[4t] and hydrosilylation[5]. Among these, carbonyl compounds' catalytic cyanosilylation produces cyanohydrins involving carbon–carbon bond formation.[6] Cyanohydrins can be easily transformed into organic and biologically important compounds, such as *α*-hydroxy acids, 1,2-diols, *α*-amino alcohols, and *β*-amino alcohols. Usually, the cyanosilylation of carbonyl compounds is carried out using trimethylsilyl cyanide (TMSCN).[3,7] In 2014, Nagendran's group used a low-valent main-group element compound, germylene cyanide (**A**), as a catalyst for the cyanosilylation of aldehydes.[8] Reports of various main-group catalysts for the cyanosilylation of aldehydes and ketones have advanced this research field.[3] Regarding Ge(II) compounds, Khan and coworkers in 2019 reported the catalytic cyanosilylation of aldehydes using non-functionalized germylene (**B**).[9] In 2021, Piskunov used *O*,*N*-heterocyclic germylene (**C**) as a catalyst for the cyanosilylation of benzaldehyde.[10] In the same year, the group of Inoue isolated a germylene cation (**D**) and used it as a catalyst for aldehyde and ketone cyanosilylation.[11] Very recently, Nembenna's group reported a *β*-dekitiminate stabilized germylene hydride (**E**) as a catalyst for the cyanosilylation of ketones.[12] To the best of our knowledge, the efficiency achieved using these germanium catalysts and other low-valent main-group catalysts [**F**,[3c] **G**,[3d] **H**,[9] and **I**[13] (Chart S1; see ESI)] has reached a TOF value of up to around 6000 h^{-1}.[11,13] Intending to find out further efficient low-valent main-group catalysts for the cyanosilylation of aldehydes and ketones, herein we report an aminotroponiminate (ATI) ligand stabilized germylene cation, [(*i*-Bu)$_2$ATIGe][B(C$_6$F$_5$)$_4$] (**2**), that provides a TOF of 15840 h^{-1} for the aliphatic aldehydes.

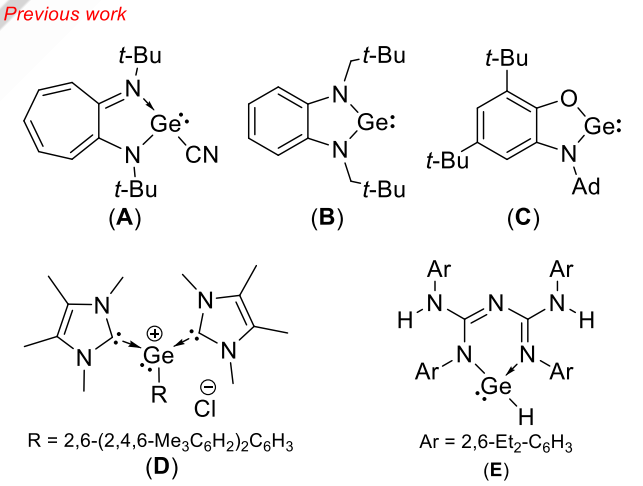

Chart 1. Germylenes (**A**–**C** and **E**) and germylene cations (**D** and **2**) used as cyanosilylation catalysts.

10.1002/asia.202400138

The ATI ligand contains a 10-electron π-system delocalized throughout the seven carbons and two nitrogen atoms. The lone pair of electrons on the nitrogen atoms provides thermodynamic stabilization, whereas the *iso*-butyl group attached to the nitrogen atoms offers kinetic stabilization.[14] Compound **2** was isolated by reacting aminotroponiminatogermylene monochloride **1** with sodium tetrakis(pentafluorophenyl)borate.

Results and discussion

Synthesis, spectra, and theoretical studies

To isolate germylene cation [(*i*-Bu)$_2$ATIGe][B(C$_6$F$_5$)$_4$] (**2**), germylene monochloride [(*i*-Bu)$_2$ATIGeCl][14] (**1**) was an apparent starting material. An equimolar reaction of compound **1** with Na[B(C$_6$F$_5$)$_4$] in DCM at −30 °C to rt for 0.5 h gave compound **2** as an air- and moisture-sensitive yellow crystalline solid in 88% yield (Scheme 1). The choice of using NaB(C$_6$F$_5$)$_4$ as a reagent for chloride abstraction instead of cheaply available NaBF$_4$ and NaBPh$_4$ is based on the observation that they do not lead to germylene cations. NaBF$_4$ showed no reaction with compound **1**, while NaBPh$_4$ reacted with compound **1**, affording compound [(*i*-Bu)$_2$ATIGe(Ph)→B(Ph)$_3$] (**2'**), an adduct of phenyl germylene with BPh$_3$ (Scheme S1; see the ESI for details).

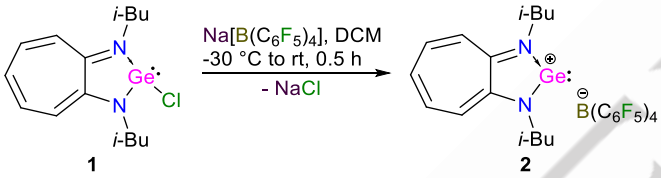

Scheme 1. Synthesis of germylene cation **2**.

Compound **2** is soluble in organic solvents such as benzene, toluene, diethyl ether, tetrahydrofuran, chloroform, and dichloromethane; however, it is insoluble in hexane and pentane. The possibility of coordinating solvents acting as Lewis bases and complexing with compound **2** was tested using THF. Adding THF to compound **2** led to a 1:1 adduct, which was confirmed by multinuclear NMR spectroscopy (see ESI). Compound **2** is stable at room temperature under a dry nitrogen atmosphere. It was characterized in solution through ^{1}H, ^{11}B, ^{13}C, and ^{19}F NMR spectroscopic studies. Since its Ge(II) atom possesses a formal cationic charge compared to the neutral Ge(II) atom in compound **1**, the electrophilicity of the germanium atom of compound **2** should be higher than that of compound **1**. Affirming this aspect, in the ^{1}H NMR spectroscopic studies, the protons of the ATI ligand of compound **2** are deshielded and appear in downfield regions compared to the corresponding peaks of compound **1**. The ^{1}H NMR spectrum of compound **2** (in CDCl$_3$) exhibited signals due to methyl, methine, and methylene protons of *iso*-butyl groups as a doublet, multiplet, and doublet at 1.09, 2.17-2.31, 4.08 ppm, respectively. The aromatic protons of the seven-membered ring were seen as a multiplet and a pseudotriplet in a 3:2 intensity ratio at 7.88-7.95 and 8.14 ppm, respectively. In its ^{11}B NMR spectrum, a signal at -16.8 ppm was observed due to the B(C$_6$F$_5$)$_4$ moiety. As anticipated, the ^{13}C NMR spectrum showed eleven signals. Its ^{19}F NMR spectrum showing signals at -132.5, -162.8, and -166.6 ppm confirms the presence of counter anion, B(C$_6$F$_5$)$_4$.

The Molecular structure of compound **2** was confirmed unambiguously by single-crystal X-ray diffraction studies (Figure 1). The single crystals of this compound were grown by the slow evaporation of its saturated solution in DCM at room temperature; the important structural parameters are shown in Table S1 (see the ESI). It crystallizes in the monoclinic space group $P2_1/n$ with two molecules in the asymmetric unit cell. Its molecular structure showed a di-coordinate germanium atom with two nitrogen atoms of the ATI ligand; the N1-Ge1-N2 bond angle is 83.36(1)°. The Ge···B distance of compound **2** is 5.287(4) Å, which suggests that the interaction between them is electrostatic.[15] The Ge-N$_{ATI}$ bonds' average length (1.873 Å) is shorter than that of compound **1** (1.938 Å). This shortening indicates that the Ge atom of compound **2** has a formal positive charge. Density Functional Theory (DFT) calculations using GAUSSIAN 09 programs support this conclusion (vide infra). Furthermore, the Gutmann-Beckett method was tried to predict the Lewis acidity of the germylene center of cation **2** (see ESI).[16] Compound **1** in CDCl$_3$ was treated with 0.25 equiv of Ph$_3$PO; the ^{31}P NMR spectrum of the resulting solution showed a peak at 29.7 ppm. Since the ^{31}P NMR spectrum of the free Ph$_3$P=O in CDCl$_3$ also peaked at 29.7 ppm, compound **1**'s germylene center has negligible Lewis acidity (Figure S24; see ESI). In contrast, the ^{31}P NMR spectrum of a mixture of compound **2** and 0.25 equiv of Ph$_3$P=O in CDCl$_3$ displayed a signal at 40.5 ppm (Figure S25; see ESI). This data reflects the significant rise in the Lewis acidity of the germylene center of compound **2** to that of compound **1**.

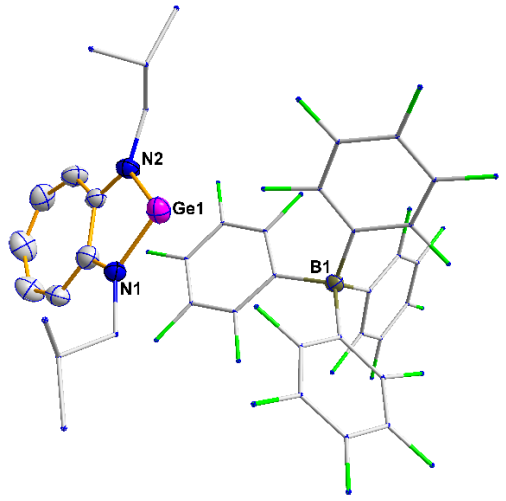

Figure 1. Molecular structure of compound **2**. Thermal ellipsoids are shown at the 30% probability level, and all hydrogen atoms are deleted for clarity. Selected bond lengths (Å) and angles (deg): Ge1···B1 5.287(4), Ge1-N1 1.886(3), Ge1-N2 1.860(3); N1-Ge1-N2 83.36(1).

DFT calculations employing hybrid B3LYP functionals were performed to understand the electronic structure of compound **2** (see ESI). The optimized geometry of compound **2** is consistent with the structure obtained by SCXRD studies. The calculations reveal two relatively strong C-F···Ge interactions (2.755 Å and 3.132 Å), somewhat stabilizing the cationic charge on the germanium center (Figure 2a). Furthermore, the ATI ligand also

10.1002/asia.202400138

RESEARCH ARTICLE

plays an essential role in stabilizing the charge. The Frontier MOs reveal that the lone pair of electrons of the germanium atom mix strongly with the π* orbital of the ligand framework (Figures 2b-c). The calculated Natural Population Analysis (NPA) charge on the germanium atom of compound **2** is significantly positive (1.23) and higher than that of compound **1** (1.08).[17] This indicates that the germanium atom of compound **2** is cationic and augments the experimental evidence (vide supra).

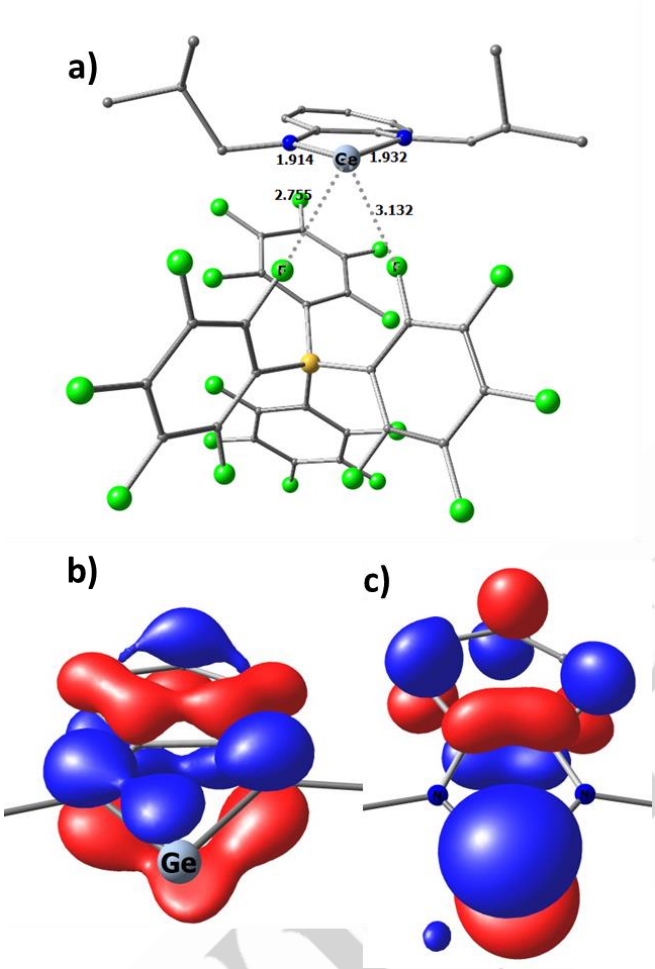

Figure 2. (a) DFT optimized geometry, (b) HOMO-8, and c) LUMO, of compound **2**. In (b) and (c), hydrogen atoms and anions are removed for clarity; further, the ^{t}Bu groups on the nitrogen atoms are only partially shown.

Apart from this, the NPA charges on the nitrogen atoms bonded to the germanium atom have significant negative charges (-0.781 and -0.785). The NBO second-order perturbation theory also reveals significant N→Ge donor-acceptor interactions (101-105 kcal/mol) that significantly localize the charge on the germanium atom. The mixing of the germanium's valence 4p orbitals with the π* orbitals of the aromatic ring further facilitates the localization. The significant energy difference between these two sets of orbitals should also be noted. Taken together, there is preferential charge accumulation on the germanium atom of compound **2**, leading to its enhanced catalytic activity (vide infra).

Cyanosilylation of aldehydes and ketones catalyzed by compound 2

Germylene cation **2** was investigated for its applicability in catalysis due to its potential Lewis acidity. The catalytic utility of compound **2** in the cyanosilylation of aldehydes and ketones using trimethylsilyl cyanide (TMSCN) under solvent-free conditions was studied; optimization reactions were carried out using benzaldehyde and acetophenone as model substrates (Table 1). The reaction of benzaldehyde with 1.1 equiv of TMSCN in the absence of a catalyst was checked at rt up to 6 h; no conversion was witnessed (entry 1; Table 1). The catalytic reaction of benzaldehyde with TMSCN using 0.05 mol% of compound **2** resulted in 68–87% conversion after 10–20 minutes at rt (entries 2–4; Table 1). Up to 99% conversion was obtained when the time was increased to 25 min (entry 5; Table 1). However, a slightly higher catalytic loading of 0.075 mol% of compound **2** gave >99% conversion in just 15 min with the TOF value 5280 h^{-1} (entry 7; Table 1). Accordingly, these conditions were selected as the optimized reaction conditions. Under the optimized reaction conditions, the catalytic efficiency of compound **1** was tested; no conversion to the product was observed (entry 8; Table 1).

Table 1. Optimization of the reaction conditions for the cyanosilylation of benzaldehyde and acetophenone using compound **2** as a catalyst

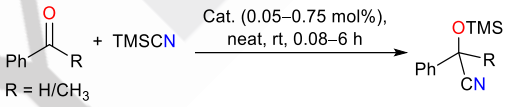

Entry	Substrate	Catalyst (mol%)	Time (h)	Conversion (%)	TOF (h^{-1})
1	PhCHO	–	6	–	–
2	PhCHO	**2** (0.05)	0.16	68	–
3	PhCHO	**2** (0.05)	0.25	78	–
4	PhCHO	**2** (0.05)	0.33	87	–
5	PhCHO	**2** (0.05)	0.41	99	4752
6	PhCHO	**2** (0.075)	0.16	95	–
7	PhCHO	**2** (0.075)	0.25	>99	5,280
8	PhCHO	**1** (0.50)	0.33	–	–
9	$PhCOCH_3$	–	6	–	–
10	$PhCOCH_3$	**2** (0.5)	0.16	93	–
11	$PhCOCH_3$	**2** (0.5)	0.25	98	–
12	$PhCOCH_3$	**2** (0.5)	0.41	>99	475
13	$PhCOCH_3$	**2** (0.75)	0.08	94	–
14	$PhCOCH_3$	**2** (0.75)	0.16	98	–
15	$PhCOCH_3$	**2** (0.75)	0.25	>99	528
16	$PhCOCH_3$	**1** (0.75)	0.33	–	–
17	$CH_3(CH_2)_2CHO$	–	0.5	–	–
18	$CH_3(CH_2)_4CHO$	–	0.5	–	–
19	PhCHO	$NaB(C_6F_5)_4$ (0.075)	0.5	–	–
20	PhCHO	$NaB(C_6F_5)_4$ (0.75)	0.25	16	–

Conditions: benzaldehyde/acetophenone (1.0 mmol), TMSCN (1.1 mmol). % Conversions were obtained by ^{1}H NMR spectroscopy; for benzaldehyde, the integration of PhC*H*O was compared with that of PhC*H*CN(OTMS). Meanwhile, for acetophenone, the integration of PhC(O)CH_3 was compared with that of PhCCN(OTMS)(CH_3). When the catalyst amount was much less, as with 0.05 mol% and 0.075 mol%, a stock solution of the catalyst in $CDCl_3$ was used. After

10.1002/asia.202400138

transferring the required amount of the catalyst solution to the reaction vessel, the solvent was removed under reduced pressure to maintain neat reaction conditions.

As aliphatic aldehydes were the most reactive ones (vide infra), the catalyst-free cyanosilylation of a few of them, namely *n*-butanal and *n*-hexanal, was also tried; these reactions did not show any conversion for 30 min (entries 17-18; Table 1). The borate salt, $NaB(C_6F_5)_4$, used in the chloride abstraction reaction of compound **1**, was also tested as a catalyst for the cyanosilylation of benzaldehyde. Under the optimized reaction conditions, no conversion was seen for up to 30 min (entry 19; Table 1). Increasing the catalyst loading to 0.75 mol% gave only 16% conversion in 15 min (entry 20; Table 1). For ketones, a similar optimization was performed using acetophenone. The reaction of acetophenone with 1.1 equiv of TMSCN without a catalyst at rt for 6 h resulted in no conversion (entry 9; Table 1). However, using 0.5 mol% of compound **2** at rt, 93, 98, and >99% conversions were seen in 10, 15, and 25 min (entries 10, 11, and 12; Table 1). Using a slightly higher catalyst loading of 0.75 mol%, >99% conversion was achieved in just 15 min with a TOF value of 528 h^{-1} (entry 15; Table 1). Under these optimized reaction conditions, compound **1** was also tested as a catalyst; however, no conversion was witnessed even up to 20 min (entry 16; Table 1).

The substrate scope for the cyanosilylation of aldehydes and ketones catalyzed by compound **2** was then studied under the optimized reaction conditions (Table 2). In the presence of 0.075 mol% catalyst, aliphatic aldehydes, such as *n*-butyraldehyde, hexanaldehyde, octanaldehyde, 3-phenylpropionaldehyde, and *trans*-cinnamaldehyde needed lesser reaction time (5 min) compared to benzaldehyde to provide >99% conversion; the TOF value is around 15,800 h^{-1} (entries 1–5; Table 2). Aromatic aldehydes with electron-withdrawing groups, such as 4-fluorobenzaldehyde and 4-chlorobenzaldehyde were cyanosilylated with >99% conversion like benzaldehyde in 15 min (entries 6–7; Table 2). 2-bromobenzaldehyde, 2-nitrobenzaldehyde, and pyridine-4-carbaldehyde were cyanosilylated slightly slower than benzaldehyde; >99% conversions were achieved in 20 min with a TOF of 3,960 h^{-1} (entries 8–10; Table 2). Pyridine-2-carbaldehyde, 3-nitrobenzaldehyde, and 4-acetylbenzaldehyde were furthermore sluggish and took 30 min to give the corresponding cyanosilylated products with a TOF of 2,640 h^{-1} (entries 11–13; Table 2). Similar to these three aldehydes, aromatic aldehydes with electron-donating groups, such as 4-methoxybenzaldehyde and 2,5-dimethoxylbenzaldehyde required higher reaction times of 30 and 35 min to afford >99% conversions; the obtained TOF values are 2,640 and 2,262 h^{-1}, respectively (entries 14–15; Table 2). Furthermore, the substrate scope for the catalytic cyanosilylation of ketones was also studied. Though the cyanosilylation rates of ketones were substantially slower than those of aldehydes, the overall reaction pattern observed with the tested aldehydes was noticed by and large with ketones. Compared to acetophenone, aliphatic ketones, such as 2-butanone, 3-methyl-2-butanone, and 4-phenyl-2-butanone, showed faster cyanosilylation, needing just 5 min in the presence of 0.75 mol% of compound **2** to produce >99% conversion with a TOF of 1,584 h^{-1} (entries 16–18; Table 2).

Aromatic ketones with electron-withdrawing groups, such as 4-fluoroacetophenone, 2-chloroacetophenone, 3-bromoacetophenone, 4-bromoacetophenone, and 4-nitroacetophenone were cyanosilylated slightly slower than acetophenone; they took 20 min to give >99% conversion with a TOF of 396 h^{-1} (entries 19–23; Table 2). Isobutyrophenone, which has an isopropyl group instead of acetophenone's methyl group, took 30 min to give >99% conversion with a TOF of 264 h^{-1} (entry 24; Table 2).

Table 2. Substrate scope for the cyanosilylation of aldehydes and ketones using compound **2** as a catalyst

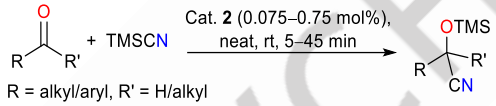

R = alkyl/aryl, R' = H/alkyl

Entry	Substrate	Cat. (mol%)	Time (min)	% conversion	% Yield (iso.)	TOF (h^{-1})
1	*n*-Butyraldehyde	0.075	5	>99	98	15,840
2	Hexanaldehyde	0.075	5	>99	98	15,840
3	Octanaldehyde	0.075	5	>99	98	15,840
4	3-Phenyl propionaldehyde	0.075	5	>99	97	15,840
5	*trans*-Cinnamaldehyde	0.075	5	>99	98	15,840
6	4-Fluorobenzaldehyde	0.075	15	>99	97	5,280
7	4-Chlorobenzaldehyde	0.075	15	>99	97	5,280
8	2-Bromobenzaldehyde	0.075	20	>99	97	3,960
9	2-Nitrobenzaldehyde	0.075	20	>99	98	3,960
10	Pyridine-4-carbaldehyde	0.075	20	>99	98	3,960
11	Pyridine-2-carbaldehyde	0.075	30	>99	98	2,640
12	3-Nitrobenzaldehyde	0.075	30	>99	97	2,640
13	4-Acetylbenzaldehyde	0.075	30	>99	98	2,640
14	4-Methoxy-benzaldehyde	0.075	30	>99	98	2,640
15	2,5-Dimethoxy-benzaldehyde	0.075	35	>99	97	2,262
16	2-Butanone	0.75	5	>99	98	1,584
17	3-Methyl-2-butanone	0.75	5	>99	98	1,584
18	4-Phenyl-2-butanone	0.75	5	>99	98	1,584
19	4-Fluoroacetophenone	0.75	20	>99	98	396
20	2-Chloroacetophenone	0.75	20	>99	97	396
21	3-Bromoacetophenone	0.75	20	>99	98	396
22	4-Bromoacetophenone	0.75	20	>99	98	396
23	4-Nitroacetophenone	0.75	20	>99	97	396
24	Isobutyrophenone	0.75	30	>99	97	264
25	4-Methoxy-acetophenone	0.75	40	>99	98	198
26	4-Methylacetophenone	0.75	45	>99	98	176

Conditions: Aldehydes/ketones (1.0 mmol), TMSCN (1.1 mmol), neat, room temperature. % Conversions were obtained by ^{1}H NMR spectroscopy; (a) for aldehydes, the integration of RC*H*O was compared with that of RC*H*CN(OTMS), and (b) for ketones, the integration of RC(O)C*H*$_3$ was compared with that of

RCCN(OTMS)(CH_3). Iso. = isolated. The TOF was calculated using % conversion. When the catalyst amount was much less, as with 0.075 mol%, a stock solution of the catalyst in $CDCl_3$ was used. After transferring the required amount of the catalyst solution to the reaction vessel, the solvent was removed under reduced pressure to maintain neat reaction conditions.

However, ketones with an electron donating group, such as 4-methoxyacetophenone and 4-methylacetophenone, were further sluggish; >99% conversions were achieved in 40 and 45 min with TOF values of 198 and 176 h^{-1}, respectively (entries 25–26; Table 2). A TOF comparison table comprising the data for all existing low-valent main-group catalysts (**A**-**I**) used for the cyanosilylation of aldehydes and ketones along with catalyst **2** shows its superiority in catalysis (Table 3). The Table lists the TOF values of a few substrates, such as *trans*-cinnamaldehyde, pyridine-4-carbaldehyde, benzaldehyde, acetophenone, 4-fluoroacetophenone, and 4-methoxy-acetophenone.

Chemoselectivity experiments

Catalyst **2** allows for inter- and intramolecular chemoselective cyanosilylation of aldehydes; one and two examples are provided for the former and latter, respectively.

Intermolecular chemoselectivity

In an equimolar reaction of benzaldehyde and acetophenone with TMSCN using 0.075 mol% of catalyst **2**, only benzaldehyde cyanosilylation occurred with 99% conversion after 0.25 h based on the ^{1}H NMR spectroscopic studies (Figure S100; see ESI). A singlet at 5.50 ppm corresponding to the -C*H*(CN)OSiMe$_3$ proton of the cyanosilylated benzaldehyde was observed along with the disappearance of a peak at 10.01 ppm for the benzaldehyde's C*H*O proton. Further, a resonance for the methyl protons of the unreacted acetophenone was seen at 2.60 ppm, and no peak at 1.86 ppm for the -C(C*H*$_3$)(CN)(OSiMe$_3$) protons of the cyanosilylated acetophenone.

Intramolecular chemoselectivity

As shown in Table 2, cyanosilylation of only the aldehydic functionality in the presence of other functional groups, such as olefin (entry 5) or ketone (entry 13), demonstrates the intramolecular chemoselectivity.

Finally, to probe the mechanism of cyanosilylation of aldehydes and ketones catalyzed by compound **2**, stoichiometric reactions of compound **2** with 2-butanone were carried out and monitored through multinuclear NMR spectroscopy. An interaction between the oxygen atom of the C=O group of 2-butanone and the Ge atom of compound **2** can be evident from the ^{1}H and ^{13}C NMR spectroscopic studies (Figures S14 and S15). In the ^{1}H NMR spectrum of the mixture of compound **2** and 2-butanone (Figure S14c), the peaks corresponding to protons of 2-butanone and the ATI ligand were slightly downfield and upfield shifted to those of free 2-butanone (Figure S14b) and compound **2** (Figure S14a), respectively. In the ^{13}C NMR spectrum (Figure S15c), the *C*=O resonance of 2-butanone (213.6 ppm) is downfield shifted compared to free 2-butanone (209.0 ppm; Figure S15b). These data reveal a weak interaction between the Lewis acidic germanium atom of compound **2** and the oxygen atom of 2-butanone, leading to an adduct or intermediate formation. No significant change was observed in the ^{11}B and ^{19}F NMR spectroscopic studies (Figures S16 and S17; see ESI).

Table 3. Comparison of the TOF (h^{-1}) values obtained (for a few substrates) using catalyst **2** with other low valent main-group catalysts **A**–**I** (used for the cyanosilylation of aldehydes and ketones)

Substrate	Catalyst[a]									
	2	**A**	**B**	**C**	**D**	**E**	**F**	**G**	**H**	**I**
trans-Cinnamaldehyde	15,840 (>99)	–	44 (88)	–	–	–	1960 (>99)	–	36 (72)	5940 (>99)
Pyridine-4-carbaldehyde	3960 (>99)	–	–	–	1900 (>99)	–	49 (>99)	–	–	–
Benzaldehyde	5280 (>99)	–	43.5 (87)	100 (75)	900 (>99)	–	588 (>99)	23 (92)	43 (86)	5940 (>99)
Acetophenone	528 (>99)	–	–	–	7 (>99)	4.2 (>99)	–	6.25 (50)	–	990 (>99)
4-Fluoroacetophenone	396 (>99)	–	–	–	6 (>99)	2.7 (>99)	–	–	–	–
4-Methoxy-acetophenone	198 (>99)	–	–	–	6.6 (>99)	2.7 (>99)	–	–	–	32.6 (98)

[a] % conversions/yields are given in brackets.

Since the efforts to crystallize and structurally characterize this intermediate were unsuccessful, a focus on isolating and structurally characterizing compounds that can mimic the intermediate's structure was made. In these attempts, the reaction of compound **2** with pyridine-*N*-oxide, which has more electron density on oxygen than that of the carbonyl's oxygen, was successful, resulting in an adduct formation, [(*i*-Bu)$_2$ATIGe←ONC$_5$H$_5$][B(C$_6$F$_5$)$_4$] (**3**) (Scheme 2). Its formation was confirmed by NMR spectroscopy and single-crystal X-ray diffraction studies. In the ^{1}H NMR spectrum of compound **3** (in $CDCl_3$), all the signals are upfield-shifted compared to the corresponding signals of compound **2**. The methyl, methine, and methylene protons of *i*-butyl groups appear as a doublet (1.05 ppm), a multiplet (2.13-2.25 ppm), and a doublet (3.62 ppm),

10.1002/asia.202400138

respectively. The five seven-membered ring protons resonate as a multiplet (7.41-7.51 ppm) and a triplet (7.73 ppm) in an intensity ratio of 4:1. The five protons of pyridine-*N*-oxide attached to the germanium center resonate as a multiplet (6.94-7.06 ppm) and a doublet (7.98 ppm) in an intensity ratio of 3:2. In the ^{11}B NMR spectrum, a signal at -16.6 ppm was observed due to $B(C_6F_5)_4$ anion. As anticipated, the ^{13}C NMR spectrum of compound **3** showed fourteen signals. In its ^{19}F NMR spectrum, signals at -132.5, -162.9, and -166.7 ppm further confirm the presence of $B(C_6F_5)_4$ anion.

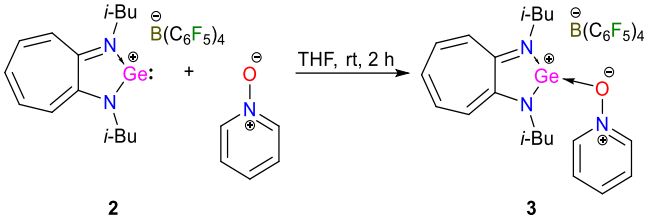

Scheme 2. Synthesis of adduct [(*i*-Bu)$_2$ATIGe←ONC$_5$H$_5$][B(C$_6$F$_5$)$_4$] (**3**).

The molecular structure of compound **3** was confirmed by single-crystal X-ray diffraction studies (Figure 3). Its single crystals were grown by the slow evaporation of its saturated solution in $CDCl_3$ and toluene mixture at room temperature. It crystallizes in the monoclinic space group $P2_1/n$. The essential structural parameters are shown in Table S1 (see the ESI). Its germanium atom is tri-coordinate with two nitrogen atoms of the ATI ligand and an oxygen atom of pyridine-*N*-oxide. The Ge···O distance (2.011(4) Å) in compound **3** is longer than the Ge-O bond of previously reported ATI ligand stabilized germylene alkoxides, which ranges from 1.872(1)Å to 1.946(4)Å.[8] This comparison confirms the weakly coordinating nature of the oxygen atom of pyridine-*N*-oxide with the germanium atom. The Ge···B distance (7.728(4) Å) in compound **3** is higher than that of compound **2**; this lengthening may be due to the stearic repulsion arising from the coordination of pyridine-*N*-oxide to the germanium atom. Due to the donation of electron density by pyridine-*N*-oxide to the germanium center of compound **3**, its Lewis acidity was anticipated to be lower than that of compound **2**. The Gutmann-Beckett method was employed to offer evidence for this (Figure S26; see ESI). The ^{31}P NMR spectrum of a mixture of compound **3** with 0.25 equivalents of Ph_3PO in $CDCl_3$ showed a signal at 33.7 ppm. As this value is lower than that of compound **2** (vide supra), the Lewis acidity of the germanium center of compound **3**, being lower than compound **2**, is revealed.

Further, to know how catalyst **2** interacts with TMSCN, stoichiometric reactions between compound **2** and TMSCN were monitored by multinuclear (^{1}H, ^{11}B, ^{13}C, ^{19}F, ^{29}Si) NMR spectroscopy. However, no significant changes were observed in the spectra (Figures S13–S17; see ESI). These studies suggest that in the catalytic reactions, aldehydes/ketones interact first with compound **2**, not the TMSCN; accordingly, a plausible mechanism is shown in Scheme 3. Catalyst **2** initiates the cycle by forming a weakly interacting adduct **2a** with an aldehyde/ketone. This intermediate **2a** reacts with trimethylsilyl cyanide (TMSCN) through a transition state **2a*** to form intermediate **2b**. During this process, the Me_3Si and CN groups of TMSCN get bonded to the oxygen and carbon atoms of the aldehyde/ketone with the cleavage of the π-bond of the C=O group, respectively.

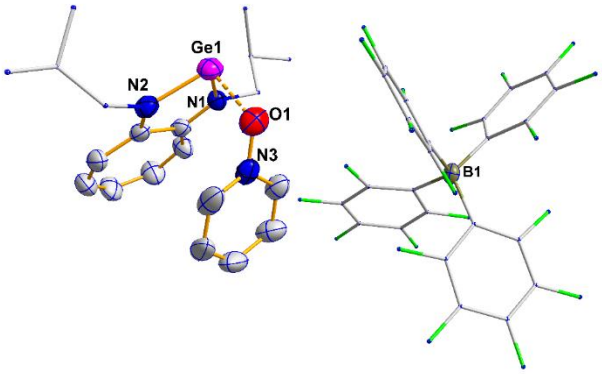

Figure 3. Molecular structure of compound **3**. Thermal ellipsoids are shown at the 30% probability level, and all hydrogen atoms are deleted for clarity. Selected bond lengths (Å) and angles (deg): Ge1···B1 7.728(4), Ge1-N1 1.917(4), Ge1-N2 1.918(3), Ge1···O1 2.011(4); N1-Ge1-N2 80.68(13).

Finally, the breakage of the weak interaction between the oxygen and germanium center in the intermediate **2b** affords the cyanosilylated product **4** and regenerates catalyst **2**.

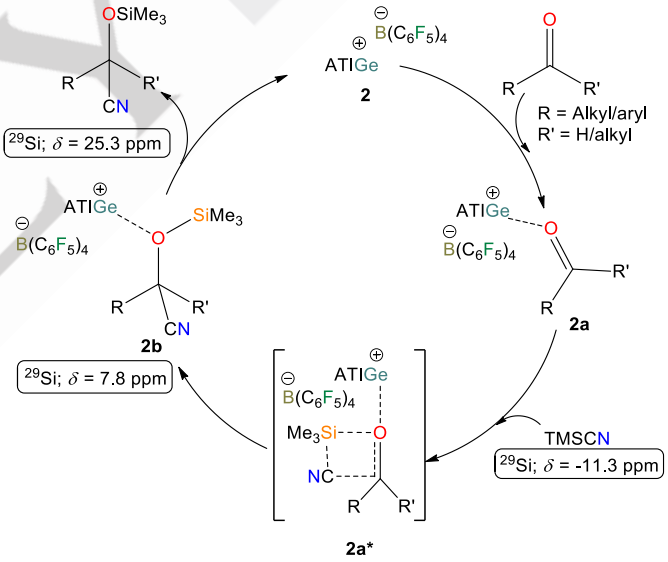

Scheme 3. Proposed mechanism for the cyanosilylation of aldehydes and ketone using TMSCN in the presence of compound **2** as a catalyst.

Conclusions

A novel ATI ligand stabilized germylene cation, [(*i*-Bu)$_2$ATIGe][B(C$_6$F$_5$)$_4$] (**2**), was successfully synthesized and characterized with its potential catalytic utility in mind. The catalytic utility of cation **2** for the cyanosilylation reactions of several aldehydes and ketones was studied. The studies have shown that compound **2** is an active cyanosilylation catalyst; the maximum TOF of ~15800 h^{-1} is seen with aliphatic aldehydes. This value is a new high for the low-valent main-group cyanosilylation catalysts. As disclosed by the DFT calculations, one of the likely reasons behind its efficient catalytic performance

10.1002/asia.202400138

could be a notable charge localization at the germanium atom. With success realized in using compound **2** as a cyanosilylation catalyst, our labs are checking the feasibility of (a) utilizing it as a catalyst for other organic transformations and (b) isolating its tin analog, again for its anticipated proficiency in elevating the potential of low-valent main-group catalysts. Furthermore, its application in small molecule activation is also being studied.

Experimental section

All experiments and manipulations were carried out in an atmosphere of dry dinitrogen using either standard Schlenk or glove box [GP(Concept)-T2, Jacomex] techniques. Solvents were dried using conventional procedures. [(*i*-Bu)$_2$ATIGeCl] (**1**) and Na[B(C_6F_5)$_4$] were prepared according to literature procedures. Pyridine-*N*-oxide was purchased from Sigma-Aldrich and was used without any further purification. TMSCN was purchased from GLR Innovations and used after distillation. All the aldehydes (except solid aldehydes) and ketones were distilled over anhydrous $MgSO_4$ before use. Melting points were measured in sealed glass capillaries using the Unitech sales digital melting point apparatus, and the reported melting points were uncorrected. ^{1}H, ^{11}B, ^{13}C, and ^{19}F spectra were recorded on a 400/500 MHz Bruker Topspin NMR spectrometer using dry $CDCl_3$. Chemical shifts (δ) are expressed in ppm. The referencing was done internally to the residual solvent and solvent resonances in the ^{1}H and ^{13}C NMR spectroscopic studies. The ^{11}B and ^{19}F spectroscopic studies used $BF_3{\cdot}Et_2O$ and $CFCl_3$ as external references, respectively. High-resolution mass spectra (HRMS) were recorded on a Waters XEVO-G2XSQTOF instrument with electrospray ionization (ESI).

Synthesis of [(*i*-Bu)$_2$ATIGe][B(C_6F_5)$_4$] (2). To a dichloromethane solution (20 mL) of compound **1** (0.50 g, 1.47 mmol), Na[B(C_6F_5)$_4$] (1.03 g, 1.47 mmol) was added at -30 °C. The reaction mixture was then brought to room temperature, stirred for 30 minutes, and filtered through a G4 frit containing celite. The solvent from the filtrate was removed under reduced pressure, resulting in compound **2** as a pale yellow solid. Yield: 1.27 g, 88%. Mp: 143 °C. ^{1}H NMR (500 MHz, $CDCl_3$): δ 1.09 (d, $^3J_{HH}$ = 6.6 Hz, 12H, CH(CH_3)$_2$), 2.17–2.31 (m, 2H, CH(CH$_3$)$_2$), 4.08 (d, $^3J_{HH}$ = 7.1 Hz, 4H, CH_2), 7.88–7.95 (m, 3H, CH), 8.14 (t, $^3J_{HH}$ = 10.5 Hz, 2H, CH) ppm; ^{13}C{^{1}H} NMR (125 MHz, $CDCl_3$): δ 20.8 (CH(*C*H$_3$)$_2$), 28.3 (*C*H(CH$_3$)$_2$), 55.3 (*C*H$_2$), 122.8, 135.3, 136.6, 137.3, 138.9, 147.3, 149.2, 158.5 (C_{Ar}) ppm; ^{11}B{^{1}H} NMR (128 MHz, $CDCl_3$): δ -16.8 (s, *B*(C_6F_5)$_4$) ppm; ^{19}F{^{1}H} NMR (470 MHz, $CDCl_3$): δ -132.5, -162.8, -166.6 ppm. HRMS (ESI-QTOF, [ATIGe]$^+$) *m/z* calc for [$C_{15}H_{23}GeN_2$] 305.1068, found 305.1054.

Synthesis of [(*i*-Bu)$_2$ATIGeONC$_5$H$_5$][B(C_6F_5)$_4$] (3). To a THF solution (20 mL) of compound **2** (0.20 g, 0.10 mmol), pyridine *N*-oxide (0.02 g, 0.22 mmol) was added at room temperature and stirred for 2 h. All the volatiles were removed under reduced pressure, resulting in compound **3** as a yellow solid. Yield: 0.21 g, 96%. Mp: 112 °C. ^{1}H NMR (500 MHz, $CDCl_3$): δ 1.05 (d, $^3J_{HH}$ = 6.5 Hz, 12H, CH(CH_3)$_2$), 2.13–2.25 (m, 2H, CH(CH$_3$)$_2$), 3.62 (d, $^3J_{HH}$ = 7.1 Hz, 4H, CH_2), 6.94–7.06 (m, 3H, CH), 7.41–7.51 (m, 4H, CH), 7.73 (t, $^3J_{HH}$ = 7.6 Hz, 1H, CH), 7.98 (d, $^3J_{HH}$ = 5.9 Hz, 2H, CH); ^{13}C{^{1}H} NMR (125 MHz, $CDCl_3$): δ 20.9 (CH(*C*H$_3$)$_2$, 27.7 (*C*H(CH$_3$)$_2$, 54.3 (*C*H$_2$), 117.1, 127.5, 135.4, 136.4, 137.3, 138.1, 139.3, 140.1, 147.3, 149.2, 160.4 (C_{Ar}); ^{11}B{^{1}H} NMR (160 MHz, $CDCl_3$): δ -16.6 (s, *B*(C_6F_5)$_4$); ^{19}F{^{1}H} NMR (470 MHz, $CDCl_3$): δ -132.5, -162.9, -166.7 ppm. HRMS (ESI-QTOF, [ATIH$_2$]$^+$) *m/z* calc for [$C_{15}H_{25}N_2$] 233.2012, found 233.2003.

General procedure for the catalytic cyanosilylation of aldehydes and ketones using compound 2 as a catalyst

Aldehyde/ketone (1.0 mmol), TMSCN (1.1 mmol), and [(*i*-Bu)$_2$ATIGe][B(C_6F_5)$_4$] (**2**) (0.075 mol% - 0.75 mol%) were mixed in an RB flask. This reaction mixture was stirred at room temperature for the required time (see Table 2). The % conversion was monitored by ^{1}H NMR spectroscopy (see the footnote of Table 2). Upon the completion of the reaction, all volatiles were removed to get a residue. It was extracted using pentane; the resultant solution was filtered, and all the volatiles were removed under a vacuum to obtain the desired product in almost analytically pure form (refer to Table 2 for the yield). For the calculation of % conversion, an aliquot (10 μL) was taken in an RB, all the volatiles were removed under reduced pressure, and ^{1}H NMR spectroscopy was recorded using the obtained residue. However, with substrates, such as *n*-butyraldehyde, hexanaldehyde, 2-butanone, and 3-methyl-2-butanone, volatiles were not removed as their boiling points were less than or equivalent to that of TMSCN. The % conversions were directly determined by ^{1}H NMR spectroscopy using the aliquot (10 μL) and hexamethyl benzene as an internal standard.

General procedure for the intermolecular chemoselective cyanosilylation using catalyst 2

Benzaldehyde (1.0 mmol), acetophenone (1.0 mmol), TMSCN (1.0 mmol), and [(*i*-Bu)$_2$ATIGe][B(C_6F_5)$_4$] (**2**) (0.075 mol %) were mixed in an RB flask and stirred at room temperature for 0.25 h. The reaction progress was monitored using ^{1}H NMR spectroscopy.

X-ray crystal structure determination of compounds 2 and 3

X-ray diffraction data of compounds **2** and **3** were collected on a Bruker SMART APEX-II CCD diffractometer (equipped with a 3-axis goniometer) using Mo Kα radiation (λ = 0.71073 Å).[18] The crystals were covered with Paratone-N and loaded on a glass fiber loop. The data were collected at room temperature or under a steady flow of cold dinitrogen. SAINT was used for data integration, and SADABS applied an empirical absorption correction.[19] The structures were solved by direct method and refined by full-matrix least-squares on F^2 using SHELXTL or SHELXL-2013 incorporated in OLEX2.[20,21] All non-hydrogen atoms were refined anisotropically; the positions of hydrogen atoms were fixed according to a riding model and were refined isotropically.

Acknowledgments

V. K. S., D. S., and P. C. J. thank the Council of Scientific and Industrial Research (CSIR), New Delhi, India, for senior research fellowships. H. K. and V. S. thanks MHRD, New Delhi, India, for the Prime Minister's Research Fellowships (PMRF). P. S. thanks,

IIT Delhi, New Delhi, India, for a senior research fellowship. S. N. thanks the SERB, Department of Science and Technology (DST), New Delhi, India, for funding (CRG/2022/005756). We thank DST-FIST (SR/FST/CSII-027/2014) and the Institute of Eminence (IOE), University Grants Commission (UGC), Ministry of Human Resource and Development, India, for establishing single crystal X-ray diffraction facilities at the Department of Chemistry, IIT Delhi. We also thank the Central Research Facility (CRF) of IIT Delhi for the NMR facility.

Keywords: Germylene • Germylene cation • Cyanosilylation • Low-valent main-group chemistry • Catalysis

References

[1] a) S. Nagendran, J. Shukla, P. Shukla, P. Mahawar, *Organometallic Compounds of Germanium*, G. Parkin, K. Meyer and D. O'Hare, *Elsevier*, Kidlington, UK, **2022**, *10*, 92–421; b) T. J. Hadlington, M. Driess, C. Jones, *Chem. Soc. Rev.* **2018**, *47*, 4176–4197; c) C. Weetman, S. Inoue, *ChemCatChem* **2018**, *10*, 4213–4228; d) S. Yadav, S. Saha, S. S. Sen, *ChemCatChem* **2016**, *8*, 486–501.

[2] P. P. Power, *Nature* **2010**, 171–177.

[3] a) N. Sen, S. Khan, *Chem. Asian J.* **2021**, *16*, 705–719; b) S. Pahar, G. Kundu, S. S. Sen, *ACS Omega* **2020**, *5*, 25477–25484; c) V. K. Singh, P. C. Joshi, H. Kumar, R. K. Siwatch, C. K. Jha, S. Nagendran, *Dalton Trans.* **2022**, *51*, 16906–16914; d) A. Karmakar, S. Hazra, G. M. D. M. Rubio, M. F. C. G. Silva, A. J. L. Pombeiro, *New J. Chem*. **2018**, *42*, 17513–17523.

[4] a) Y. Wu, C. Shan, Y. Sun, P. Chen, J. Ying, J. Zhu, L. L. Liu, Y. Zhao, *Chem. Commun.* **2016**, *52*, 13799–13802; b) J. Schneider, C. P. Sindlinger, S. M. Freitag, H. Schubert, L. Wesemann, *Angew. Chem., Int. Ed.* **2017**, *56*, 333–337; c) M. M. D. Roy, S. Fujimori, M. J. Ferguson, R. McDonald, N. Tokitoh, E. Rivard, *Chem. Eur. J.* **2018**, *24*, 14392–14399; d) Y. Liu, X. Liu, Y. Liu, W. Li, Y. Ding, M. Zhong, X. Ma, Z. Yang, *Inorg. Chim. Acta* **2018**, *471*, 244–248; e) M. Zhong, Y. Ding, D. Jin, X. Ma, Y. Liu, B. Yan, Y. Yang, J. Peng, Z. Yang, *Inorg. Chim. Acta* **2019**, *486*, 669–674; f) M. K. Sharma, M. Ansari, P. Mahawar, G. Rajaraman, S. Nagendran, *Dalton Trans*. **2019**, *48*, 664–672; g) S. Sinhababu, D. Singh, M. K. Sharma, R. K. Siwatch, P. Mahawar, S. Nagendran, *Dalton Trans*. **2019**, *48*, 4094–4100; h) V. Nesterov, R. Baierl, F. Hanusch, A. E. Ferao, S. Inoue, *J. Am. Chem. Soc*. **2019**, *141*, 14576–14580; i) K. Nakaya, S. Takahashi, A. Ishii, K. Boonpalit, P. Surawatanawong, N. Nakata, *Dalton Trans*. **2021**, *50*, 14810–14819; j) S. Pahar, V. Sharma, S. Tothadi, S. S. Sen, *Dalton Trans*. **2021**, *50*, 16678–16684; k) K. V. Arsenyeva, A. V. Klimashevskaya, K. I. Pashanova, O. Yu. Trofimova, M. G. Chegerev, A. A. Starikova, A. V. Cherkasov, G. K. Fukin, I. A. Yakushev, A. V. Piskunov, *Appl. Organomet. Chem*. **2022**, *36* (4), 1–19; l) J. Li, M. Luo, X. Sheng, H. Hua, W. Yao, S. A. Pullarkat, L. Xu, M. Ma, *Org. Chem. Front.* **2018**, *5*, 3538–3547; m) X. Cao, J. Li, A. Zhu, F. Su, W. Yao, F. Xue, M. Ma, *Org. Chem. Front.* **2020**, *7*, 3625–3632; n) L. J. Morris, P. Mahawar, J. Okuda, *J. Org. Chem.* **2023**, *88*, *8,* 5090–5096; o) K. Nakaya, S. Takahashi, A. Ishii, N. Nakata. *Inorg. Chem.* **2022**, *61* (39), 15510–15519; p) S. Stigler, S. Fujimori, A. Kostenko, S. Inoue. *Chem. Sci.* **2024**, *15*, 4275–4291; q) B. X. Leong, J. Lee, Y. Li, M. C. Yang, C. K. Siu, M. Der Su, C. W. So. *J. Am. Chem. Soc.* **2019**, *141* (44), 17629–17636; r) J. Lee, J. Fan, A. P. Koh, W. J. Joslyn Cheang, M. C. Yang, M. Der Su, C. W. So. *Eur. J. Inorg. Chem.* **2022**, *e202200129*; s) Y. C. Teo, D. Loh, B. X. Leong, Z. F. Zhang, M. Der Su, C. W. So. *Inorg. Chem.* **2023**, *62* (41), 16867–16873; t) A. Chandran, J. M. Leon Baeza, V. Timofeeva, R. Nougue, S. Takahashi, R. Ohno, A. Baceiredo, R. S. Rojas Guerrero, M. Syroeshkin, T. Matsuo, N. Saffon-Merceron, T. Kato. *Inorg. Chem.* **2022**, *61* (40), 16156–16162.

[5] a) N. D. Rio, M. Lopez-Reyes, A. Baceiredo, N. Saffon-Merceron, D. Lutters, T. Müller, T. Kato, *Angew. Chem. Int. Ed.* **2017**, *56*, 1365–1370; b) D. Sarkar, C. Weetman, S. Dutta, E. Schubert, C. Jandl, D. Koley, S. Inoue, *J. Am. Chem. Soc.* **2020**, *142*, 15403–15411; c) E. Fritz-Langhals, *ChemCatChem* **2023**,*15*, e202300442; d) Z. Zhao, J. Tan, T. Chen, Z. Hussain, Y. Li, Y. Wu, D. W. Stephan, *Inorg. Chem.* **2022**, *61*, 18670–18677.

[6] a) R. J. H. Gregory, *Chem. Rev.* **1999**, *99*, 3649–3682; b) D. L. Usanov, C. Young, M. North, *Chem. Rev.* **2008**, *108*, 5146–5226.

[7] D. A. Evans, G. L. Carroll, L. K. Truesdale, *J. Org. Chem.* **1974**, *39* (7), 914–917.

[8] R. K. Siwatch, S. Nagendran, *Chem. Eur. J.* **2014**, *20*, 13551–13556.

[9] R. Dasgupta, S. Das, S. Hiwase, S. K. Pati, S. Khan, *Organometallics* **2019**, *38*, 1429–1435.

[10] K. V. Arsenyeva, K. I. Pashanova, O. Y. Trofimova, I. V. Ershova, M. G. Chegerev, A. A. Starikova, A. V. Cherkasov, M. A. Syroeshkin, A. Y. Kozmenkova, A. V. Piskunov, *New J. Chem.* **2021**, *45*, 11758–11767.

[11] D. Sarkar, S. Dutta, C. Weetman, E. Schubert, D. Koley, S. Inoue, *Chem. Eur. J.* **2021**, *27*, 13072–13078.

[12] A. P. Khuntia, N. Sarkar, A. G. Patro, R. K. Sahoo, S. Nembenna, *Eur. J. Inorg. Chem.* **2022**, e202200209.

[13] W. Wang, M. Luo, J. Li, S. A. Pullarkat, M. Ma, *Chem. Comm.* **2018**, *54* (24), 3042–3044.

[14] R. K. Siwatch, S. Kundu, D. Kumar, S. Nagendran, *Organometallics* **2011**, *30*, 1998–2005.

[15] Y. Xiong, T. Szilvási, S. Yao, G. Tan, M. Driess, *J. Am. Chem. Soc*. **2014**, *136* (32), 11300–11303.

[16] P. Erdmann, L. Greb, *Angew. Chem. Int. Ed.* **2022**, *61*, e202114550.

[17] M. K. Sharma, S. Sinhababu, D. Yadav, G. Mukherjee, G. Rajaraman, S. Nagendran, *Chem. – Asian J.* **2018**, *13*, 1357–1365.

[18] SMART: Bruker Molecular Analysis Research Tool, Version 5.618; Bruker AXS: Madison, WI, **2000**.

[19] SAINT-NT, Version 6.04; Bruker AXS: Madison, WI, **2001**.

[20] SHELXTL-NT, Version 6.10; Bruker AXS: Madison, WI, **2000**.

[21] a) O. V. Dolomanov, L. J. Bourhis, R. J. Gildea, J. A. K. Howard, H. Puschmann, OLEX2: A complete structure solution, refinement and analysis program, *J. Appl. Crystallogr.* **2009**, *42*, 339–341; b) G. M. Sheldrick, *Acta Cryst.* **2015**, *C71*, 3–8.

[22] Deposition numbers 2329111 (**2**), 2329112 (**3**), and 2348211(**2'**) https://www.ccdc.cam.ac.uk/services/structures?id=doi:10.1002/asia.202400138 contain supplementary crystallographic data for this paper. These data are provided free of charge by the joint Cambridge Crystallographic Data Centre and Fachinformationszentrum Karlsruhe http://www.ccdc.cam.ac.uk/structures Access Structures service.

10.1002/asia.202400138

WILEY VCH

RESEARCH ARTICLE

Entry for the Table of Contents

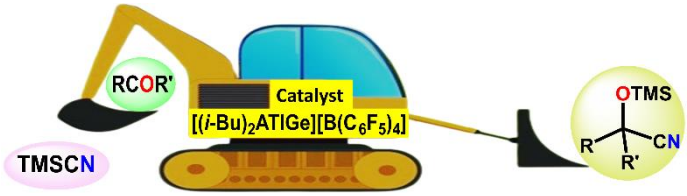

A novel ATI ligand-stabilized germylene cation [(*i*-Bu)$_2$ATIGe][B(C$_6$F$_5$)$_4$] (**2**) has been identified as an efficient catalyst for the cyanosilylation of aldehydes and ketones. The TOF it offers for aliphatic aldehydes (15,800 h^{-1}) shows the potential of low-valent main-group element compounds in catalysts. (ATI = aminotroponiminate, TOF = turnover frequency).

Institute and researcher Twitter usernames: @Chemistry_iitd and @SNagendranGroup